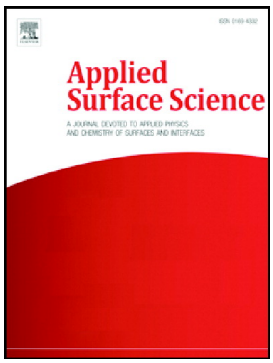

Use of image analysis to evaluate surface dispersion and covering performance of nanolime coatings sprayed on heritage material substrates

Marcos Lanzón, Victoria E. García-Vera, Antonio Tenza-Abril, Valerio De Stefano

PII: S0169-4332(19)30678-6
DOI: https://doi.org/10.1016/j.apsusc.2019.03.066
Reference: APSUSC 42021

To appear in: *Applied Surface Science*

Received date: 8 November 2018
Revised date: 22 February 2019
Accepted date: 7 March 2019

Please cite this article as: M. Lanzón, V.E. García-Vera, A. Tenza-Abril, et al., Use of image analysis to evaluate surface dispersion and covering performance of nanolime coatings sprayed on heritage material substrates, Applied Surface Science, https://doi.org/10.1016/j.apsusc.2019.03.066

Use of image analysis to evaluate surface dispersion and covering performance of nanolime coatings sprayed on heritage material substrates.

Marcos Lanzón[1], Victoria E. García-Vera[1], Antonio Tenza-Abril[2], Valerio De Stefano[1]

[1] Departamento de Arquitectura y Tecnología de la Edificación, Universidad Politécnica de Cartagena, 30203 Cartagena, Spain / e-mail: marcos.lanzon@upct.es

[2] Department of Civil Engineering, University of Alicante, Alicante, Spain

Abstract:

Coatings are often used to reinforce the surface of monuments, although little is known about their surface dispersion and effectiveness. This paper examines the surface distribution of $Ca(OH)_2$ nanoparticle-based coatings ($Ca(OH)_2$-NP). The coatings were sprayed on different substrates and studied by image analysis software and microscopy. Using image segmentation techniques the phase of interest (coating) was separated from the background material and evaluated. In control surfaces, up to 92.73% of the examined area was coated by the nanoparticles. In contrast, when the treatment was sprayed on building materials the NP-coatings were preferentially deposited in weaker zones, such as cracks or defects of the surface. In this case, the processed images revealed that less than 30% of the examined surface was coated by the NP-coating.

Keywords: Nanoparticles deposition; consolidating coatings; segmentation; image analysis; non-destructive tests; heritage materials

1. Introduction

Protective coatings are necessary to extend the durability of ancient materials **[1-3]**. For instance, the use of nanoparticle-based $Ca(OH)_2$ alcoholic suspensions has been recently reported in consolidating stucco, adobe and stone surfaces **[4]**. An advantage of the treatment is that the small size of the nanoparticles facilitates their penetration through the pore system of mechanically-weak materials. Besides, the waiting time between consecutive coats is considerably reduced because of the volatility of alcohols in comparison with conventional solutions as lime water **[5]**. The mechanical reinforcement of the surface is explained by conversion of $Ca(OH)_2$ into $CaCO_3$ by atmospheric CO_2, a process also referred to as *carbonation* **[6]**. Since the vast majority of ancient materials are eminently calcareous, the new $CaCO_3$ coating is highly compatible with the substrate. In fact, the substrate-coating similarity is an important concern in conservation science as the original surface should not be altered **[7]**.

Coatings with consolidating features delay the surface weathering reducing its maintenance. However, the coating performance should be evaluated by reliable and preferably non-destructive methods. The peeling test provides useful information about the cohesion and consolidation of grains partially detached on the surface. The test, which produces minimal damage, uses adhesive strips to remove small amounts of material generally of the order of milligrams or less **[8]**. On the contrary, more aggressive techniques like laser devices are used for effective cleaning and patina removing in heritage objects **[9]**, marble and sandstone **[10-12]**. Microscopy examination has provided

valuable information on the efficacy of cleaning and the intrinsic characteristics of the surface **[13-16]**. However, the homogenous distribution of the coating, and therefore its effectiveness, has been scarcely addressed since it is not exempt from practical difficulties. In SEM analysis, for example, the phase of interest (coating) might be difficult to distinguish due to its poor contrast with the substrate. This problem is more evident when $Ca(OH)_2$-NP coatings are spread on rather similar substrates, as for instance calcitic surfaces, as they are converted into $CaCO_3$ **[4]**.

Non-destructive techniques are gaining importance in the diagnosis of heritage materials. This paper aims to develop new methodologies for evaluating coatings' performance using microscopy, image analysis and segmentation. First, the coating is deposited and tested on control surfaces that are rather different from the coating. The images acquired with the microscope were uploaded in the software ImageJ to perform thresholding and segmentation operations. Building materials were also studied to ascertain whether their irregular surface had an influence on the homogenous distribution of the coating. It was found that the consolidant was preferentially accumulated on weaker areas of the substrate, which is an advantage for its successful consolidation. In addition, the covering capacity was quantified with the software providing data that are consistent with microscopy examination.

2. Materials and methods

2.1. Synthesis of $Ca(OH)_2$-NP

Pure $Ca(OH)_2$-NP were synthesised in a glass reactor under N_2 atmosphere to prevent carbonation to happen (Fig. 1a). The reaction was carried out using analytical grade reagents and the purification of the solid phase was carried out as recently described by Madrid and Lanzón **[17]**:

$NaOH + CaCl_2 \rightarrow Ca(OH)_2 \downarrow + NaCl$

After that, suspensions of 5 g/L were prepared dispersing pure $Ca(OH)_2$ in 2-propanol and sonicated to obtain stable mixtures. The flasks were purged with nitrogen, closed and sealed with Parafilm® to extend the durability of the suspension.

2.2. TEM and SEM examination

The $Ca(OH)_2$-NP were examined by TEM to study morphological aspects and the range size of the nanoparticles. First, the liquid was diluted ten times with 2-propanol (0.5 g/L) and 5 µl were deposited on 200 mesh grids. Then, the drop was left for several minutes in the grids to achieve total evaporation of 2-propanol. TEM examination was conducted at 200 kV with a JEOL JEM-2100 microscope and the images were saved as .tiff files.

Scanning Electron Microscopy (SEM) was used to assess the thickness of nanoparticle-based $Ca(OH)_2$ coatings sprayed on flat surfaces (control). The control surface consisted of 40x40 mm black cellulose substrates on which the treatment was repeatedly sprayed. The coating was applied at a uniform distance of 10 cm in five consecutive layers with a laboratory nebuliser (Fig. 1b). Once coated, the control surfaces were metallised with Au (25 nm coating)

to increase the image quality as usual in secondary electrons mode. The SEM microscope (Hitachi S-3500N) was operated at ultra-high vacuum and an accelerating voltage of 5kV.

2.3. Optical microscopy

A Digital Microscopy (Dino-Lite Edge) for surface examination was used to characterise the coatings deposited on the surface. The microscope was equipped with Dino-Capture 2.0 software, polariser filter and a measurement device that allows precise quantification of distances at the selected magnification (Fig. 2). A set of adjustable LEDs allowed adjustment of light intensity and hence, the acquisition of comparable images with the microscope. The images were captured at the same magnification (65x), saved as .tiff files and opened with ImageJ software.

2.4. Image analysis & segmentation: physical distribution of NP-coatings

ImageJ 1.50i software was used to evaluate the coatings distribution on the surface of control and building material samples. This software has been used for the characterisation of a number of materials like wood and stone in the context of heritage conservation **[18-20]**. First, the scale bar at the bottom of the image was used to calibrate the image i.e. to transform pixel distances into physical distances. Once calibrated, the images were converted into 8-bits images, from which grayscale histograms were displayed. As expected, white coatings as calcite provided a narrow peak on the right part of the histogram, whereas the black substrate gave an intense peak on the left side. A number of algorithms are available in ImageJ for thresholding images. In this case, the

chosen algorithm was IsoData (Iterative Self Organising Data Analysis) **[21-22]**. Finally, the segmented images were processed to evaluate the coating area relative to the total area.

2.5. Peeling tests and hardness: consolidation efficiency of NP-coatings

The surface cohesion of treated and non-treated samples was studied by means of non-destructive methods like peeling tests and hardness (Fig. 3). The peeling test was carried out with 10 x 50 mm adhesive strips on the external surface of laboratory-made plasters (Fig. 3.a). The material adhered to the tape was weighed with a resolution of ±0.0001g **[8]**. The measurements were repeated 10 times to calculate the average amount of material bonded to the strip (removed) as well as the relative standard deviation (RSD %).

The study of consolidation was completed with a Baxlo® durometer suitable for soft materials (Fig. 3b). The durometer uses a truncated cone indenter to create small indentations on the surface. The hardness was measured 10 times per sample and a standard material (60 Shore-A units) was used as reference.

3. Results

3.1. Morphological study of $Ca(OH)_2$-NP

The use of analytical grade reagents in the synthesis ($CaCl_2$ and NaOH) facilitated formation of pure $Ca(OH)_2$-NP. TEM examination confirmed the nanoparticles were hexagonal in shape as expected for pure portlandite crystals (Fig 4) **[17]**. The dimensional characteristics of portlandite 2D nanoparticles were studied with ImageJ. First, the images were calibrated in nm using the

scale-bar displayed at the bottom and the known distance was converted from pixels into nm. The diameter of $Ca(OH)_2$ nanoparticles was calculated from the line segments that run between vertices of the hexagons (Fig. 4a). The measurement was conducted on ten nanoparticles (numbered as 1-10 in Fig. 4b) and the average size was 386.2 nm. A number of NPs, for example NP #10 and nearby ones, had diameters around 30-40 nm and were, therefore, considerably smaller in size.

The control 40x40 mm surfaces were stored under laboratory conditions for 28 days to ensure complete carbonation of the coatings to happen ($CaCO_3$). After that, they were examined by SEM to assess the coating thickness resulting from applying five layers of treatment (Fig. 4c-d). SEM images showed valuable information on carbonated coatings (yellow arrows) deposited on the cellulosic structure of control surfaces (white arrows). The coating deposition was somewhat uniform, although some NPs clusters were formed on the surface (Fig. 4c). Further examination along the paper-coating transition zone, revealed the maximum thickness of the coating was around 15 µm, as shown in Fig. 4d.

3.2. Coating-substrate separation

The use of segmentation allowed the separation of the NP coating from the control substrate. In 8-bits images, the grayscale varies from 0 (black objects) to 255 (white objects), thus giving a total of 256 graylevels. Optical microscopy images were converted into 8-bits, calibrated in mm and processed with ImageJ (Fig. 5). The histograms corroborated that coating (white) and substrate (black) gave well-resolved peaks and therefore, distinguishable from one another (Fig. 5a). Furthermore, the software discriminates between dense

NP coatings, moderately coated and non-coated areas based on their grayscale levels.

In the control surface, the left zone was intentionally left uncoated to study the grayscale variation from left to right. A region of interest (ROI) was drawn across non-coated and coated zones of the surface and grayscale data were plotted against the calibrated distance, in mm (Fig. 5a). The plot shows consistent information as densely-coated areas provided higher grayscale values as compared to moderately-coated or non-coated areas (Fig. 5b).

3.3. Evaluating the covering performance of nanolime coatings

Since the software is able to extract reliable information on the coating, further analyses were performed to assess the covering efficiency of nanolime. Considering that the left part of the substrate in Fig. 6a was not treated with nanolime, the coating surface represents 67.04% of the examined area. Besides, the binary images show practical information about non-coated zones (defects) that might be connected to the application method (Fig. 6b). However, in coated substrates the covering performance must be higher as the left part of the surface was not treated with nanolime as earlier commented.

To test the reliability of the method, the analysis was repeated in fully-coated samples using equivalent grayscale ranges (Fig. 6c). Equally, the foreground coating was segmented to measure the percentage of treatment deposited on the studied surface. Fig. 6d shows that some zones were rather well coated since fewer defects were found in the images. In this case, the covering performance was increased up to 92.73% of the total examined area.

3.4. Assessing the coating's performance on heritage materials

Earthen materials were chosen in the study as they are often used in heritage constructions and need consolidation. Laboratory-made samples were confectioned with clay, sand and water to obtain a workable paste that was plastered and smoothed with a trowel **[22-24]**. Besides, a small fragment taken from the reconstruction of an earthen-wall in The Alhambra was used to evaluate the treatment in real heritage samples.

It was found that the NPs were mainly accumulated in weaker zones of the surface, such as the binder-aggregate Interfacial Transition Zone (Fig. 7). The particular spread pattern of $Ca(OH)_2$ NPs might be connected to differential suction of the substrate. The heterogeneous distribution of the coating and its accumulation in certain zones was confirmed by image analysis. In fact, in the studied earthen plasters the coating covered less than 10-12% of the surface.

Similarly, The Alhambra fragment was treated with nanolime to examine the coating distribution pattern (Fig. 8). In this case, to investigate the influence of the deposition method, small volumes (20 µL each) were carefully applied with a micropipette. In comparison with the sprayer, the NPs concentration was higher as the deposition takes place on a rather small area. The colour images confirmed the irregular distribution of the coating when a single injection of nanolime was performed (Fig. 8a). Once again border grains and tiny cracks were apparently filled and strengthened with $Ca(OH)_2$-NPs. Image segmentation confirmed the covered area was lower than 8.5% of the computed area (Fig. 8b). The analysis was repeated in several zones, but the coating's distribution rarely exceeded 10% of the examined area. Finally, the consolidant

was applied three times with the micropipette on the same point to saturate the surface (Fig. 8c). The threshold process and histogram is shown in Fig. 8d using the same grayscale interval to separate coating and background. The impregnation was repeated in different zones and the coating distribution was around 28-30% relative to the examined area.

3.5. Testing the consolidation efficiency of nanolime coatings

Table 1 shows erosion and hardness data obtained by peeling tests and Shore-A durometers conducted on earthen plasters. As expected, the consolidation efficiency notably differs for peeling and Shore-A tests since they are aimed to obtain information on the surface erosion and indentation, respectively. In the peeling tests, the degree of material removed by adhesion was considerably reduced by a factor of 4.7 in consolidated samples. The consolidation efficiency (78.9%) was calculated as percent variation between coated and non-coated samples. Shore-A data equally confirmed the surface reinforcement of NP-coated samples when comparted to non-coated ones.

Conclusions

- Image analysis and segmentation is a suitable method in non-destructive diagnosis of heritage materials. ImageJ provides valuable information to evaluate essential requirements on the practicability of coatings. For example, the number of layers necessary to ensure a given performance can be evaluated by image analysis.

- The reliability of the analysis is greatly improved when nanolime coatings are applied on black surfaces. In these conditions, coating and background are clearly separated in the histogram, allowing precise quantification of both phases. With the proposed method i.e. five coats (5g/L), sprayed with nebuliser at constant distance (10 cm), the nanolime coating covered up to 92.73 % of the substrate. Although laboratory experiments are not fully comparable to field conditions, the outcomes might be useful when similar coatings were applied on monuments and buildings.
- The coating distribution is most likely affected by inherent features of the surface. In fact, the treatment is preferentially accumulated in critical zones of the surface, such as pores, defects and grain borders. Therefore, the consolidant may reinforce weak areas and zones that are prone to deterioration in the long-term. The selective filling of consolidant in critical zones could be partially explained by the higher suction of pores and cracks on the surface. However, further research is needed to elucidate the particular mechanisms behind such behaviour.
- Finally, it is worth stressing that despite the diluted nature of the suspensions (5g/L), physical measurements conducted on the surface of earthen plasters prove the consolidating effect of nanolime coatings.

References

[1] G. Graziani, E. Sassoni, E. Franzoni, G.W. Scherer, Hydroxyapatite coatings for marble protection: optimization of calcite covering and acid resistance, Appl. Surf. Sci. 368 (2016) 241–257.

[2] C. Rodriguez-Navarro, A. Suzuki, E. Ruiz-Agudo, Alcohol Dispersions of Calcium Hydroxide Nanoparticles for Stone Conservation Alcohol dispersions of calcium hydroxide nanoparticles for stone conservation, Langmuir 29 (2013) 11457–11470.

[3] P. Meloni, F. Manca, G. Carcangiu, Marble protection: an inorganic electrokinetic approach, Appl. Surf. Sci. 373 (2013) 377–385.

[4] M. Lanzón, J.A. Madrid, A. Martínez-Arredondo, S. Mónaco, Use of diluted $Ca(OH)_2$ suspensions and their transformation into nanostructured $CaCO_3$ coatings: A case study in strengthening heritage materials (stucco, adobe and stone), Appl. Surf. Sci. 424 (2017) 20–27.

[5] E. Doehne, C.A. Price, Stone Conservation an Overview of Current Research, The Getty Conservation Institute, Los Angeles, California, 2010.

[6] C. Rodríguez-Navarro, E. Ruiz-Agudo, Nanolimes: from synthesis to application, Pure Appl. Chem. 90 (2018) 523-550.

[7] E. Hansen, E. Doehne, J. Fidler, J. Larson, B. Martin, M. Matteini, C. Rodriguez-Navarro, E. Sebastián Pardo, C. Price, A. de Tagle, J.M. Teutonico, N. Weiss, A review of selected inorganic consolidants and protective treatments for porous calcareous materials, Rev. Conserv. 4 (2003) 13–25.

[8] ASTM D3359-08, Standard Test Methods for Measuring Adhesion by Tape Test, ASTM International 2008.

[9] A.V. Rode, K.G.H. Baldwin, A. Wain, N.R. Madsen, D. Freeman, Ph. Delaporte, B. Luther-Davies, Ultrafast laser ablation for restoration of heritage objects, Appl. Surf. Sci. 254 (2008) 3137-3146.

[10] P. Maravelaki-Kalaitzaki, V. Zafiropulos, C. Fotakis, Excimer laser cleaning of encrustation on Pentelic marble: procedure and evaluation of the effects, Appl. Surf. Sci. 148 (1999) 92–104.

[11] S. Klein, F. Fekrsanati, J. Hildenhagen, K. Dickmann, H. Uphoff, Y. Marakis, V. Zafiropulos, Discoloration of marble during laser cleaning by Nd:YAG laserwavelengths, Appl. Surf. Sci. 171 (2001) 242–251.

[12] S. Klein, T. Stratoudaki, Y. Marakis, V. Zafiropulos, K. Dickmann, Comparative study of different wavelengths from IR to UV applied to clean sandstone, Appl. Surf. Sci. 157 (2000) 1–6.

[13] A.L. Damas, Maria do Rosário Veiga, P. Faria, A. Santos Silva, Characterisation of old azulejos setting mortars: A contribution to the conservation of this type of coatings, Constr. Build. Mater. 171 (2018) 128-139.

[14] M.L. Weththimuni, M. Licchelli, M. Malagodi, N. Rovella, M. La Russa, Consolidation of bio-calcarenite stone by treatment based on diammonium hydrogenphosphate and calcium hydroxide nanoparticles, Measurement 127 (2018) 396-405.

[15] V. Daniele, G. Taglieri, R. Quaresima, The nanolimes in Cultural Heritage conservation: Characterisation and analysis of the carbonation process, J. Cult. Herit. 9 (2008) 294-301.

[16] I. Natali, M.L. Saladino, F. Andriulo, D.C. Martino, E. Caponetti, E. Carretti, Luigi Dei, Consolidation and protection by nanolime: Recent advances for the conservation of the graffiti, Carceri dello Steri Palermo and of the 18th century

lunettes, SS. Giuda e Simone Cloister, Corniola (Empoli), J. Cult. Herit. 15 (2014) 151-158.

[17] J.A. Madrid, M. Lanzón, Synthesis and morphological examination of high-purity $Ca(OH)_2$ nanoparticles suitable to consolidate porous surfaces, Appl. Surf. Sci. 424 (2017) 2–8.

[18] G.B. Goffredo, B. Citterio, F. Biavasco, F. Stazi, S. Barcelli, P. Munafò, Nanotechnology on wood: The effect of photocatalytic nanocoatings against Aspergillus niger, J. Cult. Herit. 27 (2017) 125-136.

[19] D. Miriello, G.M. Crisci, Image analysis and flatbed scanners, A visual procedure in order to study the macro-porosity of the archaeological and historical mortars, J. Cult. Herit. 7 (2006) 186-192.

[20] O. Rozenbaum, E. Le Trong, J.L. Rouet, A. Bruand, 2-D image analysis: A complementary tool for characterizing quarry and weathered building limestone, J. Cult. Herit. 8 (2007) 151-159.

[21] T.W. Ridler, S. Calvard, Picture thresholding using an iterative selection method, IEEE Transactions on Systems, Man and Cybernetics 8 (1978) 630-632.

[22] V.E. García-Vera, M. Lanzón, Physical-chemical study, characterisation and use of image analysis to assess the durability of earthen plasters exposed to rain water and acid rain, Constr. Build. Mater. 187 (2018) 708-717.

[23] E. Hamard, J. C. Morel, F. Salgado, A. Marcom, N. Meunier, A procedure to assess the suitability of plaster to protect vernacular earthen architecture, J. Cult. Herit. 14 (2) (2013) 109-115.

[24] R. Deliniere, J.E. Aubert, F. Rojat, M. Gasc-Barbier, Physical, mineralogical and mechanical characterization of ready-mixed clay plaster, Build. Environ. 80 (2014) 11-17.

Fig. 1 a) Glass reactor and modified atmosphere to avoid carbonation; b) compressor and laboratory nebuliser containing nanoparticles in 2-propanol (5 g/L)

Fig. 2. Digital microscope for surface examination. Accessories, calibration device and example of 40x40 mm control surface.

Fig. 3 Test for measuring the physical resistance of materials at the surface: a) adhesive strips for peeling tests; b) Shore-A durometer for soft materials.

Fig. 4. TEM and SEM examination: a) use of ImageJ to measure the size of 2D $Ca(OH)_2$ NPs; b) the NPs were perfectly hexagonal and the calculated average size was 386.2 nm; c) $CaCO_3$ coating after carbonation of $Ca(OH)_2$; d) cross-section of coating with a thickness of 13.9 µm.

Fig. 5. Transition zone between control surface (black) and $Ca(OH)_2$-NP coating sprayed in five consecutive layers; a) background and coating give separate peaks in the histogram; b) ROI showing discrimination between non-coated areas (left part), moderately coated areas (central part) and densely coated ones (right part).

Fig. 6. Segmentation process: a) Control substrate partially coated with nanolime; b) binary image showing foreground objects in black (phase of interest); c) dense nanolime coating on control surface; d) nanolime coating covering 92.73% of the surface.

Fig. 7. Laboratory-made earthen samples coated with nanolime. Left image: The coating is more concentrated along grain borders, weaker zones and pores (arrows); Right image: foreground objects (coating) analysed by the software in the examined area.

Fig. 8. Heritage material, 1.5 cm size fragment, taken from a wall under reconstruction in The Alhambra: a) colour images showing grain borders filled and reinforced with NPs by injecting 1x20 µL (white phase); b) binary image showing nanolime segmentation in black; c) Injection of 3x20 µL of nanolime suspension on the same fragment; d) threshold and histogram to separate the coating (red).

Table 1. Consolidation efficiency in laboratory-made earthen materials

	Peeling test, µg/cm^2			Shore-A hardness, %		
	Non-coated material	NP-coated material	Consolidation efficiency, %	Non-coated material	NP-coated material	Consolidation efficiency, %
Average	954.6	201.6	78.9	81.4	92.3	13.4
Sigma[1]	100.34	20.88		4.62	4.69	
RDS%	10.51	10.36		5.68	5.08	

[1] ten repetitions were made per sample (n=10)

Highlights

Image analysis is a suitable method to evaluate the surface dispersion of coatings

Nanolime 5g/L covered 92.73% of the surface when sprayed in 5 coats (10 cm distance)

The coating distribution was affected by inherent features of the substrate (surface)

Image examination reveals the consolidant is mainly accumulated in cracks and defects

The methodology is non-destructive and, therefore, appropriate for Heritage Materials

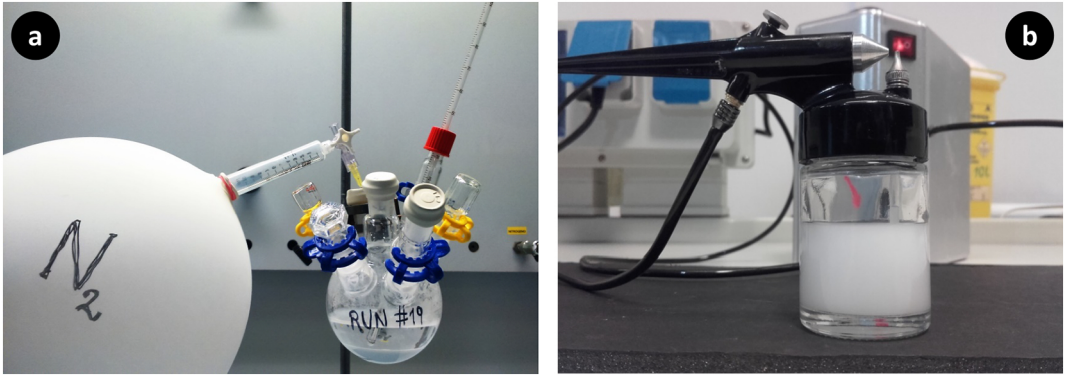

Figure 1

Figure 2

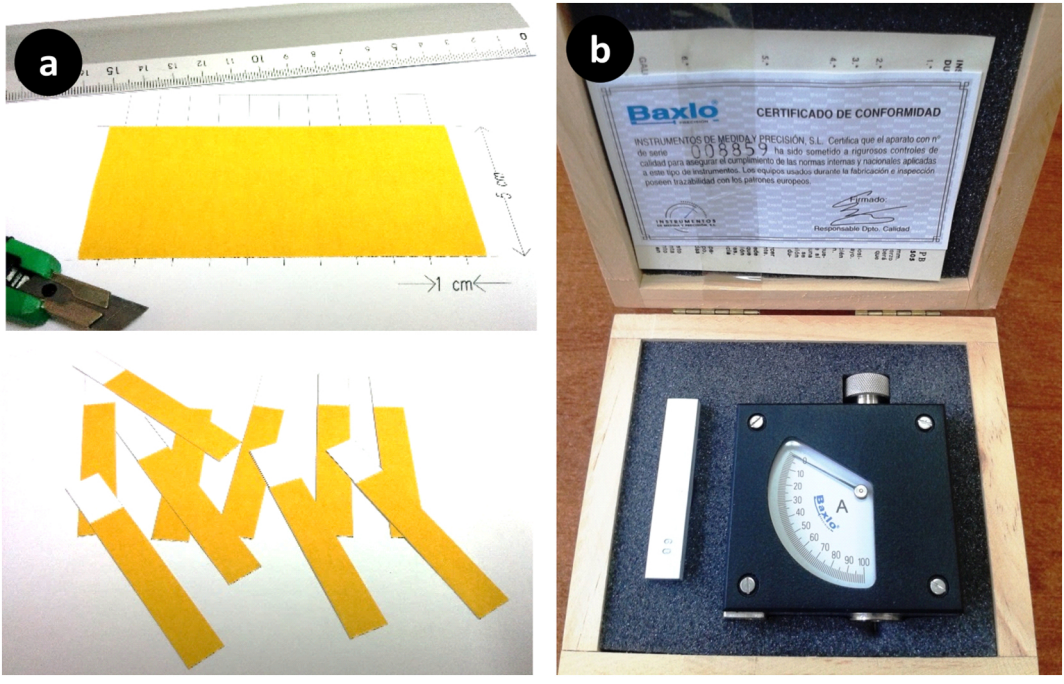
a
1 cm
b
Baxlo
CERTIFICADO DE CONFORMIDAD
INSTRUMENTOS DE MEDIDA Y PRECISIÓN, S.L. Certifica que el aparato con nº de serie 008859 ha sido sometido a rigurosos controles de calidad para asegurar el cumplimiento de las normas internas y nacionales aplicadas a este tipo de instrumentos. Los equipos usados durante la fabricación e inspección poseen trazabilidad con los patrones europeos.
Firmado:
Responsable Dpto. Calidad
Baxlo
A

Figure 3

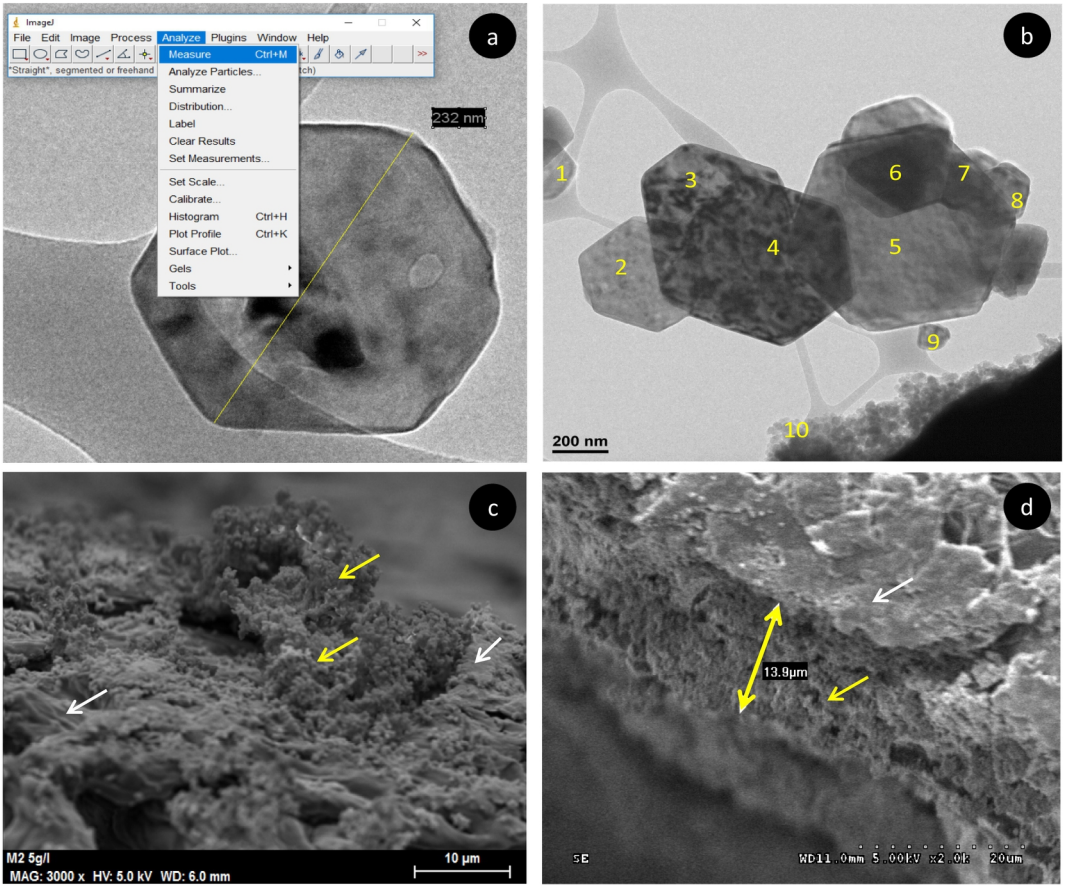
a
ImageJ
File Edit Image Process Analyze Plugins Window Help
Measure Ctrl+M
Analyze Particles...
Summarize
Distribution...
Label
Clear Results
Set Measurements...
Set Scale...
Calibrate...
Histogram Ctrl+H
Plot Profile Ctrl+K
Surface Plot...
Gels
Tools
232 nm
b
1
2
3
4
5
6
7
8
9
10
200 nm
c
M2 5g/l
MAG: 3000 x HV: 5.0 kV WD: 6.0 mm
10 µm
d
13.9µm
SE
WD11.0mm 5.00kV x2.0k 20um

Figure 4

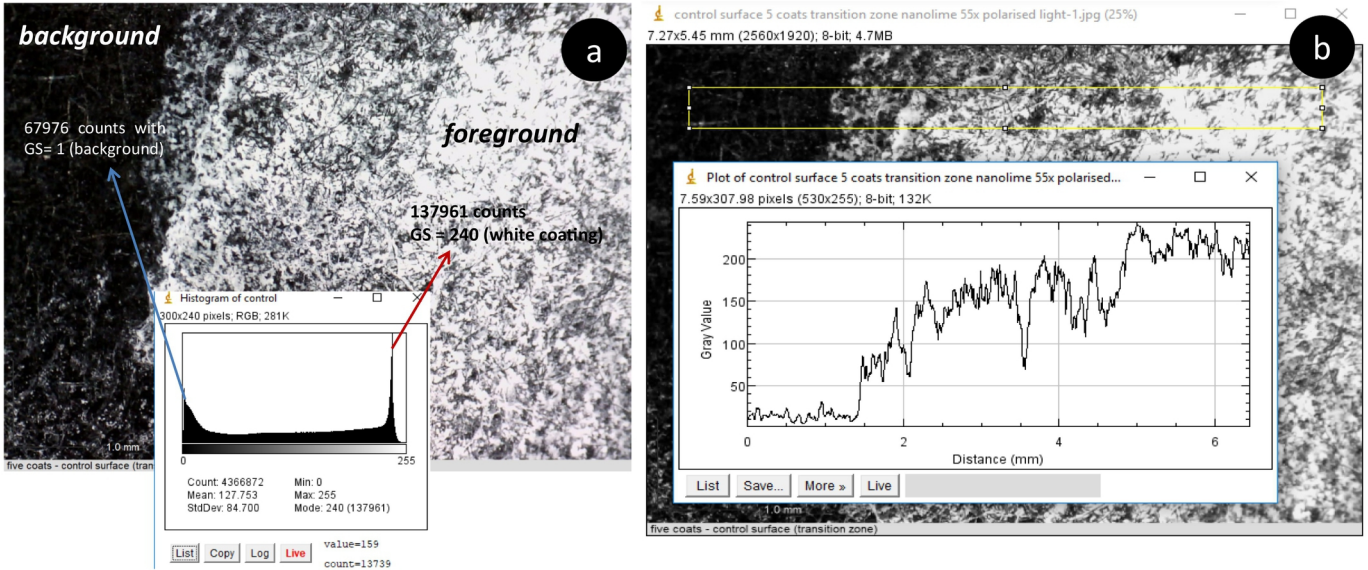
background
a
67976 counts with
GS= 1 (background)
foreground
137961 counts
GS = 240 (white coating)
Histogram of control
300x240 pixels; RGB; 281K
0
255
Count: 4366872
Mean: 127.753
StdDev: 84.700
Min: 0
Max: 255
Mode: 240 (137961)
List
Copy
Log
Live
value=159
count=13739
1.0 mm
five coats - control surface (tran
control surface 5 coats transition zone nanolime 55x polarised light-1.jpg (25%)
7.27x5.45 mm (2560x1920); 8-bit; 4.7MB
b
Plot of control surface 5 coats transition zone nanolime 55x polarised...
7.59x307.98 pixels (530x255); 8-bit; 132K
Gray Value
200
150
100
50
0
2
4
6
Distance (mm)
List
Save...
More »
Live
1.0 mm
five coats - control surface (transition zone)

Figure 5

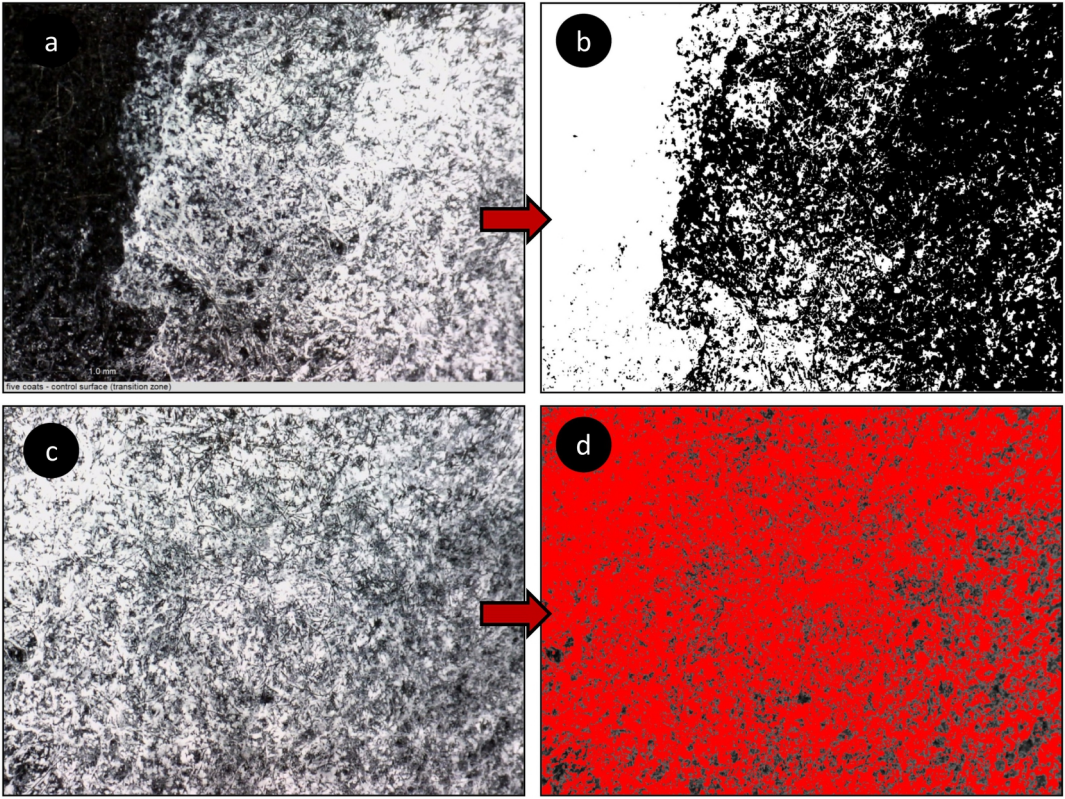

Figure 6

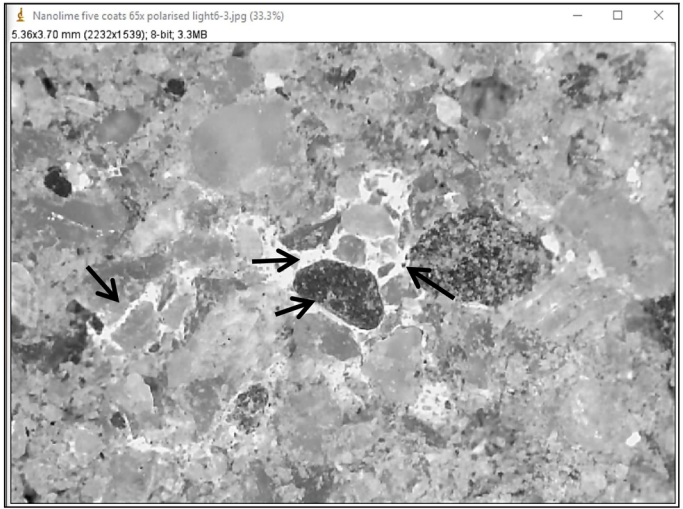
Nanolime five coats 65x polarised light6-3.jpg (33.3%)
5.36x3.70 mm (2232x1539); 8-bit; 3.3MB

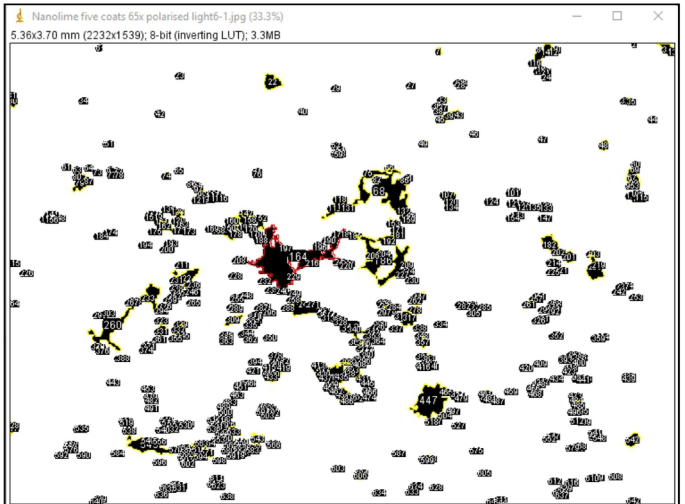
Nanolime five coats 65x polarised light6-1.jpg (33.3%)
5.36x3.70 mm (2232x1539); 8-bit (inverting LUT); 3.3MB

Figure 7

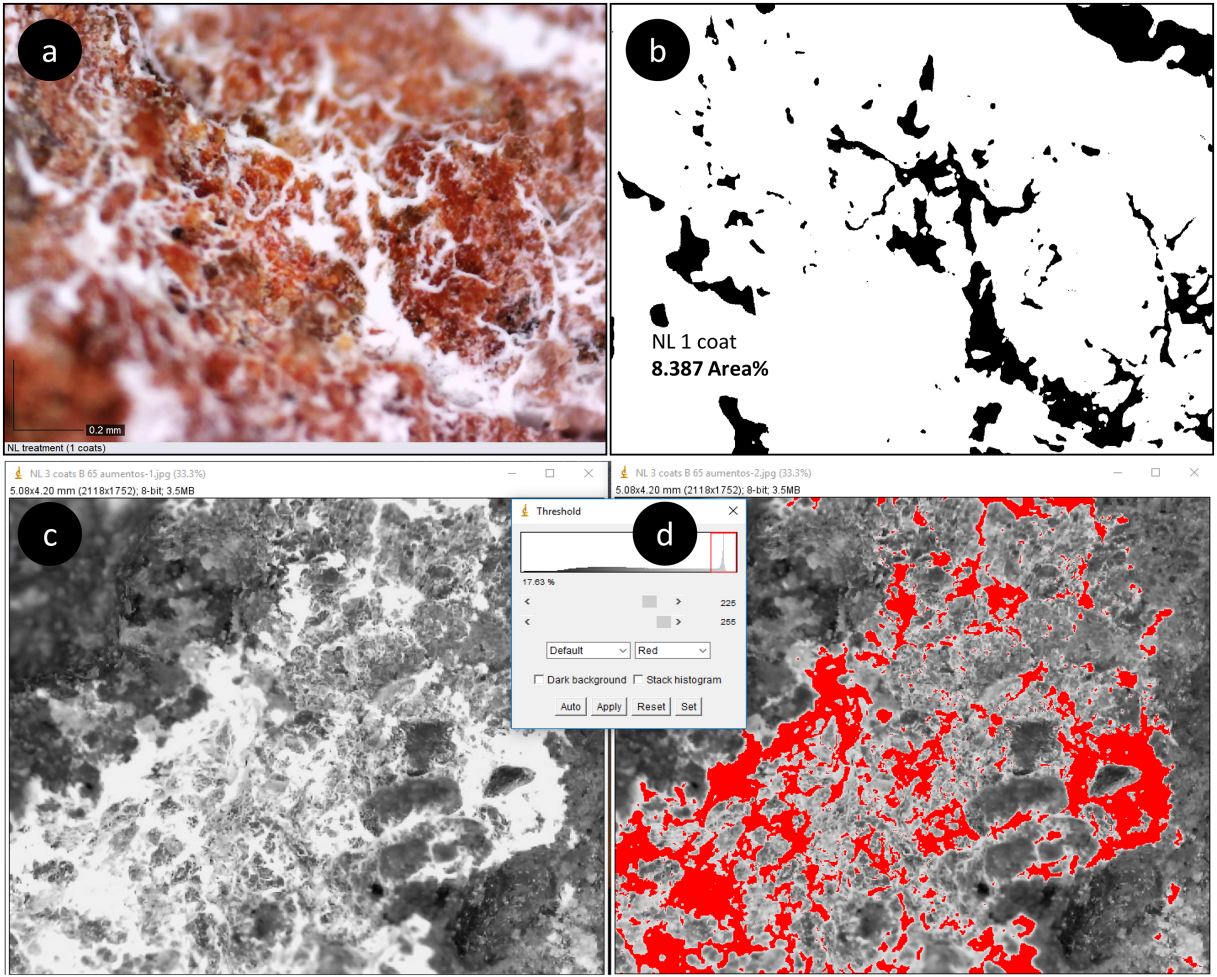
a
0.2 mm
NL treatment (1 coats)
b
NL 1 coat
8.387 Area%
NL 3 coats B 65 aumentos-1.jpg (33.3%)
5.08x4.20 mm (2118x1752); 8-bit; 3.5MB
c
NL 3 coats B 65 aumentos-2.jpg (33.3%)
5.08x4.20 mm (2118x1752); 8-bit; 3.5MB
Threshold
d
17.63 %
225
255
Default
Red
Dark background
Stack histogram
Auto
Apply
Reset
Set

Figure 8